Magnetism and exchange in the layered antiferromagnet $NiPS_3$

1994 J. Phys.: Condens. Matter 6 4569

(http://iopscience.iop.org/0953-8984/6/24/017)

J. Phys.: Condens. Matter 6 (1994) 4569–4579. Printed in the UK

Magnetism and exchange in the layered antiferromagnet $NiPS_3$

Nirmala Chandrasekharan and Sukumaran Vasudevan

Department of Inorganic and Physical Chemistry, Indian Institute of Science, Bangalore 560 012, India

Received 1 September 1993, in final form 28 February 1994

Abstract. The anisotropic susceptibility of the layered antiferromagnet $NiPS_3$ (T_N = 155 K) has been measured between 45 K and 650 K. The system may be described by the effective spin Hamiltonian $\mathcal{H} = DS_{iz}^2 - \sum_{ij} J_{ij} S_i \cdot S_j$, with the quadratic single-ion anisotropy terms introducing anisotropy in an otherwise isotropic situation. The exchange J and single-ion anisotropy parameter D were determined from an analysis of the anisotropic susceptibility data for two different models: (i) the Oguchi model, in which a pair of spins chosen at random is treated exactly while its interactions with the rest of the crystal are approximated by a mean field and (ii) the correlated effective field (CEF) approximation developed by Lines, which reduces the many-body problem to a single-particle, non-interacting ensemble form, by the introduction of static temperature-dependent correlation parameters, which are evaluated by forcing consistency with the fluctuation–dissipation theorem. It is found that the CEF approximation is superior to the Oguchi model in describing the susceptibility of $NiPS_3$. The exchange and crystal field parameters for the CEF approximation are $J/k = -58.0$ K; $D/k = 16.1$ K; $g_\parallel = 2.05$ and $g_\perp = 2.13$.

1. Introduction

There has been continuing interest in low-dimensional magnetic systems, because of the variety of phenomena that they exhibit [1, 2]. Among the known low-dimensional systems, the layered transition metal chalcogenophosphates, MPX_3 (M = Mn, Fe, Ni and X = S, Se) are rather unique; they represent one of the few known layered systems in which both magnetic and crystallographic lattices are two dimensional (2D). Unlike most other 2D magnetic systems, wherein magnetic layers are separated by diamagnetic layers, in the transition metal thiophosphates, the MPX_3 layers are separated by a van der Waals gap. The presence of the gap rules out super-exchange pathways and since the inter-layer metal–metal distance is of the order of $\sim$ 6.5 Å, direct exchange too would be negligible; the chalcogenophosphates are hence nearly 'perfect' 2D magnetic systems, with the metal ions forming a honeycomb arrangement within the layer. An interesting consequence of the van der Waals gap is that it is possible to intercalate a wide variety of guest molecules and ions as in the case of transition metal dichalcogenides. Subsequent to intercalation there are considerable changes in magnetic behaviour [3–6]. An obvious prerequisite to understanding these changes is a quantitative evaluation of the exchange and crystal field parameters of the host. In this paper we have attempted to do this for $NiPS_3$, from an analysis of the susceptibility data.

$NiPS_3$ like the other transition metal thiophosphates orders antiferromagnetically at low temperatures [7, 8]. These materials are ionic insulators, the transition metal d electrons

0953-8984/94/244569+11$19.50

localized and atomic like and the d electron manifold adequately described in the weak-field limit of crystal field theory [9].

An interesting feature of magnetism in the transition metal thiophosphates is that the anisotropy in the magnetism is strongly dependent on the metal ion. The anisotropy in the transition metal thiophosphates has been shown to originate from crystal field effects [8], as a consequence of the zero-field splitting of the M^{2+} ion d levels [10], due to the trigonal distortion of the MS_6 octahedra. Thus in the case of $NiPS_3$, the $^3A_{2g}$ ground state of an octahedrally coordinated Ni^{2+} is split under the combined action of the trigonal distortion and spin–orbit coupling, to give a doublet and a singlet separated by D.

The effective spin Hamiltonian which describes the system is

$$\mathcal{H} = -\sum_{ij} J\boldsymbol{S}_i \cdot \boldsymbol{S}_j + \sum_i DS_{iz}^2 \tag{1}$$

with D introducing anisotropy in an otherwise isotropic situation.

In this paper we report an analysis of the anisotropic susceptibility of $NiPS_3$. In low-dimensional systems such as $NiPS_3$ it is well known that spin correlations persist at temperatures much higher than T_N [1] and consequently the simple mean field approximation (MFA), which completely ignores these correlations, is likely to be a poor approach. At the same time the zero-field splitting of the Ni^{2+} d levels, which is of the order of kT, makes it difficult to apply more refined theories [11]. In analysing the susceptibility, we have used two different models which try and incorporate an element of spin correlation,while at the same time retaining the simplicity of the molecular field approximation. The two are (i) the Oguchi molecular field [12, 13] in which a pair of spins chosen at random from the crystal is treated exactly while the coupling of this pair with the rest of the spins in the crystal is approximated by an effective field and (ii) the correlated effective field (CEF) developed by Lines [11], in which the effective field felt by an ion is approximated by the sum of the ensemble average of the rest of the spins and a term proportional to the instantaneous deviation of the spin from its own ensemble value. The temperature-dependent proportionality constant appearing in the latter term, which is a measure of the static correlations, is determined by forcing the model to be consistent with the fluctuation–dissipation theorem.

The susceptibility for an $S = 1$ ion with uniaxial quadratic anisotropy has been derived for the above two models. The zero-field splitting parameter D and the exchange integral J were evaluated by fitting the theoretical expression to the experimental susceptibilities.

In 2D magnetic systems wherein exchange is isotropic or has an XY anisotropy, transitions to long-range order arise as a consequence of weak 3D inter-layer coupling (e.g. dipolar coupling). In such situations, it is unlikely that models which are used to describe the 2D high-temperature susceptibility would be able to predict the correct transition temperatures.

2. Experimental details

$NiPS_3$ was synthesized from the corresponding elements and single crystals grown by chemical vapour transport using excess sulphur as the transporting agent [3].

Magnetic susceptibility measurements were made on a Faraday magnetic balance. Temperatures in the range 45–300 K were obtained using a closed cycle cryostat (Air Products). Measurements in the temperature range 300–650 K were performed using a high-temperature furnace assembly. The susceptometer was calibrated using Hg $[Co(NCS)_4]$ as

a standard. The crystals were suspended from the balance by an arrangement similar to that reported in [14]. The arrangement allowed the measurements of susceptibilities for different orientations of the crystal with respect to the field. The susceptibilities reported are for two directions—the field parallel and perpendicular to the trigonal axis. The trigonal axis in $NiPS_3$ is perpendicular to the layers.

The susceptibilities were corrected for the diamagnetic as well as the temperature-independent paramagnetic (TIP) contributions. The TIP contributions for the $^3A_{2g}$ ground state of Ni^{2+} is given by $8N\mu_B^2/10$ Dq [15]. Optical absorption studies [9] had reported a 10 Dq value of 8900 cm^{-1} for $NiPS_3$. The TIP contribution is thus 0.235×10^{-3} emu mol^{-1}.

3. Results and discussion

The temperature variation of the susceptibility of $NiPS_3$ for the two directions—parallel and perpendicular to the trigonal axis—is shown in figure 1. The data are identical to the results obtained from measurements made on a vibrating sample magnetometer [8]. In the paramagnetic phase ($T > 155$ K) $\chi_\perp > \chi_\parallel$, whereas below $T_N = 155$ K it may be seen that the magnetization axis of the antiferromagnetic state is perpendicular to the trigonal axis.

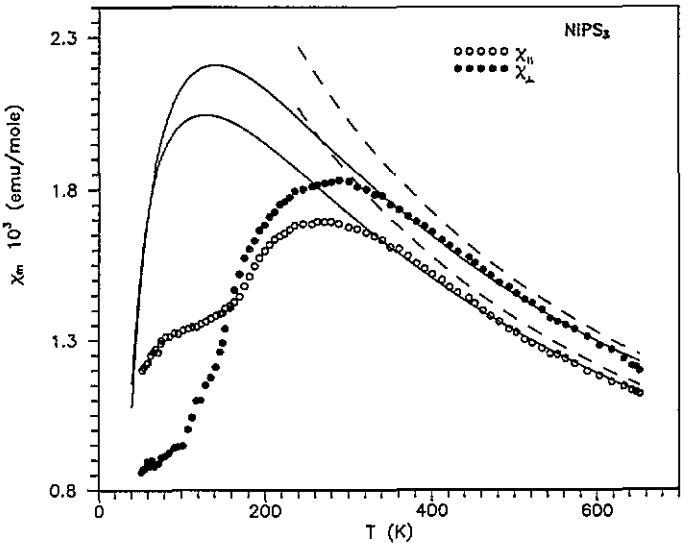

Figure 1. Magnetic susceptibility of $NiPS_3$ single crystals parallel ($\chi_\parallel$) and perpendicular ($\chi_\perp$) to the trigonal axis as a function of temperature. The solid lines are the fit of the anisotropic susceptibility expression in the Oguchi model (equations (5) and (6)) for $J/k = -66.9$ K; $D/k = 16.3$ K; $g_\parallel = 2.06$ and $g_\perp = 2.14$. The broken lines are the anisotropic susceptibilities calculated in the MF approximation for the same value of the exchange and crystal field parameters as in the Oguchi approximation.

The anisotropy in the susceptibilities is a consequence of the zero-field splitting of the $^3A_{2g}$ ground state of Ni^{2+} by the trigonal distortion. The fact that $\chi_\perp > \chi_\parallel$ directly implies a splitting of the ground-state triplet into a lower singlet and an upper doublet (figure 2). The isolated ion may be represented by the Hamiltonian $\mathcal{H} = DS_{iz}^2$. For $NiPS_3$, D is positive. The anisotropy is weak since the splitting of the $^3A_{2g}$ state by the trigonal field is an indirect

effect, arising from the spin–orbit coupling of the $^3A_{2g}$ state with the higher-lying $^3T_{2g}$ state, whose degeneracy is lifted by the trigonal distortion. The exchange parameter J and the zero-field splitting D were estimated over the entire temperature range of the experimental susceptibility, within the Oguchi model as well as the correlated effective field theory of Lines.

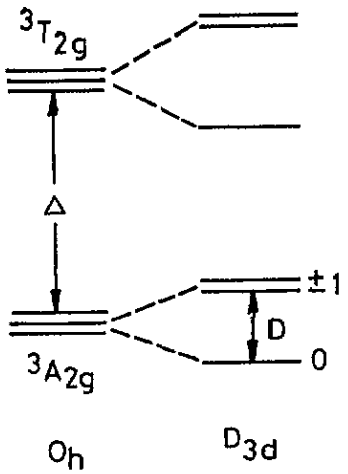

Figure 2. The splitting of the Γ_5 ($^3A_{2g}$ and $^3T_{2g}$) for a d^8 ion under the influence of a trigonal field. Δ is the crystal-field splitting and D is the zero-field splitting.

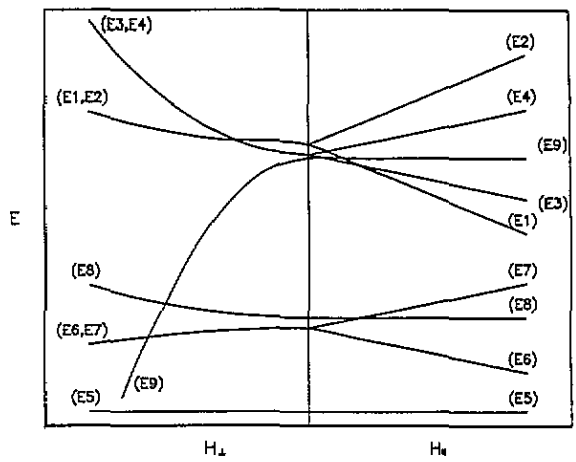

Figure 3. The Zeeman splitting for an Ni^{2+} dimer in an external field applied parallel and perpendicular to the trigonal axis. The D and J values are those which give the best fit to the Oguchi model ($D/k = 16.3$ K; $J/k = -66.9$ K). The labelling of the states is as referred to in the appendix.

3.1. Oguchi model

This is one of the simpler models which incorporates an element of spin correlations into the MFA. Interactions between neighbouring magnetic ions are treated exactly while the interactions of the pair with the rest of the lattice are approximated by a molecular field. The magnetic Hamiltonian for such a pair is

$$\mathcal{H} = D[S_{1z}^2 + S_{2z}^2] - 2J[S_1^z S_2^z + (S_1^+ S_2^- + S_1^- S_2^+)] - \mathcal{H}_{\text{Zeeman}}$$

$$\mathcal{H}_{\text{Zeeman}} = g_{\|}\beta H_{\text{eff}}^{\|}(S_1^z + S_2^z) - \tfrac{1}{2}g_{\perp}\beta H_{\text{eff}}^{\perp}(S_1^+ + S_2^+ + S_1^- + S_2^-). \qquad (2)$$

In equation (2) z, $\|$, coincides with the trigonal axis and

$$H_{\text{eff}} = H^0 + H_{\text{Ogu}}$$

where H_{Ogu} (the field is due to all the other magnetic ions) is proportional to the magnetization

$$H_{\lambda\text{Ogu}} = \frac{2(z-1)JM_\lambda}{Ng_\lambda^2\beta^2} \qquad \lambda = \|, \perp . \qquad (3)$$

As the pair was chosen at random, its average magnetic moment per atom must be the same as that of any other pair and consequently the same as that of the entire crystal. We require, for consistency, that the magnetization along any axis λ be

$$M_\lambda = Ng_\lambda\beta\frac{\langle S_\lambda\rangle_{\text{dimer}}}{2}. \tag{4}$$

The derivation of $\langle S_\parallel\rangle_{\text{dimer}}$ and $\langle S_\perp\rangle_{\text{dimer}}$ for an Ni^{2+} pair ($S_1 = S_2 = 1$) with single-ion quadratic anisotropy terms is straightforward. The energies of the dimer (see the appendix) in the field were obtained by treating the $\mathcal{H}_{\text{Zeeman}}$ in equation (2) as a perturbation. The energy diagram for an $S = 1$ dimer in an external field is shown in figure 3.

The average spin moments $\langle S_\lambda\rangle_{\text{dimer}}$ are calculated from the pair partition function, $Z_\lambda = \sum_i e^{-\epsilon_i/kT}$, according to the relation

$$\langle S_\lambda\rangle_{\text{dimer}} = \frac{kT}{g_\lambda\beta}\frac{\delta \ln Z_\lambda}{\delta H}.$$

The expressions for $\langle S_\parallel\rangle$ and $\langle S_\perp\rangle$ are given in the appendix. The magnetization along the different axes may be obtained by substitution of $\langle S_\lambda\rangle_{\text{dimer}}$ in equation (4) and zero-field directional susceptibilities, $M_\lambda/H_{\lambda,0}$, may be obtained by rearranging the terms. The expressions for the susceptibilities are

$$\chi_{\text{Ogu}\parallel} = \frac{M_\parallel}{H^0} = \frac{Ng_\parallel^2\beta^2}{kT}\left[\frac{4e^{4J-D/kT} + e^{4J/kT} + 1}{G(J,D,T) - 2(z-1)(J/kT)(4e^{4J-D/kT} + e^{4J/kT} + 1)}\right] \tag{5}$$

$$\chi_{\text{Ogu}\perp} = \frac{M_\perp}{H^0} = \frac{Ng_\perp^2\beta^2F(J,D,T)}{G(J,D,T) - 2(z-1)JF(J,D,T)} \tag{6}$$

$$G(J,D,T) = 2e^{4J-D/kT} + 2e^{4J/kT} + 2 + e^{J+\gamma/kT} + e^{J-\gamma/kT} + e^{-D/kT}$$

$$F(J,D,T) = D^{-1}(-2e^{4J-D/kT} + 2e^{4J/kT} + 1 - e^{-D/kT}) + \frac{3C_2^2}{3J-\gamma}(e^{4J/kT}e^{J+\gamma/kT})$$

$$+ \frac{3C_1^2}{3J+\gamma}(e^{4J/kT}e^{J-\gamma/kT}).$$

The parameters C and γ have been defined in the appendix. The $J, D, g_\parallel$ and $g_\perp$ parameters were determined for the Oguchi model by fitting the expressions to the experimental data using the method of least squares. The best fits, shown in figure 1 as the full lines, are for $J/k = -66.9$ K, $D/k = 16.3$ K, $g_\parallel = 2.06$ and $g_\perp = 2.14$. In the fitting program J, D and $g_\parallel$ were floated. $g_\perp$ is related to $g_\parallel$ by the relation $g_\perp = g_\parallel + 2D/|\lambda|$ [16]. The value of $|\lambda| \simeq 280$ cm^{-1} was taken from [9].

For comparison, the MFA suceptibilities are shown as the broken lines in figure 1. The expression for the MFA susceptibility is

$$\chi_{\lambda\text{MFA}} = \frac{\chi_\lambda^0}{1 - 2zJ\chi_\lambda^0/Ng_\lambda^2\beta^2} \tag{7}$$

where χ_λ^0 are the isolated ion susceptibilities [10] and are

$$\chi_\perp^0 = \frac{Ng_\perp^2\beta^2}{kT}\frac{(2kT/D)(1 - e^{-D/kT})}{1 + 2e^{-D/kT}} \tag{8}$$

and

$$\chi_\parallel^0 = \frac{Ng_\parallel^2\beta^2}{kT}\frac{2e^{-D/kT}}{1 + 2e^{-D/kT}}. \tag{9}$$

It may be seen from figure 1 that, as expected, the Oguchi model improves upon the MFA.

3.2. Correlated effective field

The CEF formalism proposed by Lines [11] is ideally suited for systems wherein the magnetic Hamiltonian can be written in the form

$$\mathcal{H} = \mathcal{H}_{\text{CF}} + \mathcal{H}_{\text{exchange}}. \tag{10}$$

$\mathcal{H}_{\text{CF}}$ is the Hamiltonian in the absence of exchange.

This has been employed with reasonable success in analysing the susceptibility of the one-dimensional $RbFeBr_3$ [17] and $RbFeCl_3$ [18] where, as in the present case, $\mathcal{H}_{\text{CF}} = \sum_i D S_{iz}^2$. In the case of the isotropic Heisenberg lattice where $D = 0$ and the orbital angular momentum is completely quenched, the results of the CEF model tally exactly with the results of the random phase Green function approximation [11]. The CEF model attempts to reduce the many-body problem to a single-body, non-interacting ensemble form, by the introduction of static temperature-dependent spin correlation parameters α^λ ($\lambda = \parallel$ or $\perp$), which are evaluated by forcing consistency with the fluctuation–dissipation theorem.

In this model, the correlated effective field for the ith spin, S_i, is obtained by replacing each S_j in equation (1) by the sum of two contributions, one its ensemble average $\langle S_j \rangle$, the other a term proportional to the instantaneous deviation of S_i from its own averaged value $\langle S_i \rangle$ i.e.

$$S_j^\lambda \longrightarrow \langle S_j^\lambda \rangle + \alpha^\lambda (S_i^\lambda - \langle S_i^\lambda \rangle). \tag{11}$$

Corresponding to this replacement, the effective Hamiltonian for the ith spin in the high-temperature paramagnetic phase is

$$\mathcal{H}_i^0(\text{eff}) = D(S_{iz}^2) \sum_{j\lambda} 2 J_{ij}^\lambda \alpha^\lambda (S_i^\lambda)^2. \tag{12}$$

In the presence of an applied field H^0 in the direction λ

$$\mathcal{H}_i(\text{eff}) = \mathcal{H}_i^0(\text{eff}) - g\beta H_0 S^\lambda + 2 \sum_{j\lambda} J_{ij}^\lambda S_i^\lambda (\langle S_j^\lambda \rangle - \alpha^\lambda \langle S_i^\lambda \rangle). \tag{13}$$

The field-dependent ensemble averages are obtained by treating the last two terms in equation (13) as a perturbation on $\mathcal{H}_i^0(\text{eff})$. The field-dependent ensemble averages are

$$kT \langle S(q)^\lambda \rangle_H = Hg\beta \langle S_i^\lambda : S_i^\lambda \rangle_0 + 2[J(q)^\lambda - \alpha^\lambda J^\lambda(0)] \langle S(q)^\lambda \rangle_H \langle S_i^\lambda : S_i^\lambda \rangle_0 \tag{14}$$

where $S(q)$ and $J(q)$ are the Fourier transforms of the corresponding lattice quantities and the momentum q belongs to the first Brillouin zone.

The colon product ensemble average is defined by

$$\langle S_i^\lambda : S_i^\lambda \rangle_0 = \sum_n \rho_n \left(S_{nn}^\lambda S_{nn}^\lambda + 2kT \sum_{m \neq n} \frac{S_{nm}^\lambda S_{mn}^\lambda}{E_m - E_n} \right). \tag{15}$$

S_{nm}^λ are the matrix elements of the λth component of the ith spin between the nth and mth eigenstates, E_n and E_m are the eigen energies of the respective levels and ρ_n is the density matrix. The susceptibility defined by $\chi_i^\lambda(q) = N\langle S(q)^\lambda \rangle / H$ may be written as

$$kT \chi_i(q)^\lambda = g_\lambda^2 \beta^2 \langle S_i^\lambda : S_i^\lambda \rangle_0 + U^\lambda(q) \tag{16}$$

where

$$U^{\lambda}(q) = \frac{2[J(q) - \alpha^{\lambda} J(0)]\langle S_i^{\lambda} : S_i^{\lambda}\rangle_0^2}{kT - 2[J(q) - \alpha^{\lambda} J(0)]\langle S_i^{\lambda} : S_i^{\lambda}\rangle_0}. \tag{17}$$

From the fluctuation theorem we have $\sum_q U(q) = 0$ [11] which allows the complete determination of the correlation parameters, α^{λ}. Once α^{λ} is obtained the uniform static susceptibility directly follows as

$$\chi_0^{\lambda} = \frac{N g_{\lambda}^2 \beta^2 \langle S_i^{\lambda} : S_i^{\lambda}\rangle_0}{kT - 2zJ(0)(1 - \alpha^{\lambda})\langle S_i^{\lambda} : S_i^{\lambda}\rangle_0} \tag{18}$$

where z is the coordination number around the central metal ion.

For an antiferromagnet (AFM) the Néel temperature—the temperature at which the staggered susceptibility, χ ($q = q^*$; q^* is the antiferromagnetic ordering vector) diverges—may be calculated in the CEF model as the temperature at which the denominator of equation (18) goes to zero for $q = q^*$. Noting that for an AFM $J(q^*) = -J(0)$ it follows that the Néel temperature, T_N, is

$$kT_N = 2zJ(0)(1 + \alpha^{\lambda})\langle S_i^{\lambda} : S_i^{\lambda}\rangle_0. \tag{19}$$

The susceptibilities of $NiPS_3$ were calculated using equation (18), after evaluation of the α parameters from equation (17). The equations for α^{λ} involve a summation over the Brillouin zone. We have used the special 'k' point scheme of Chadi and Cohen [19] for obtaining the averages over the Brillouin zone. For $NiPS_3$ where the Ni^{2+} ions form a honeycomb lattice the $6k$ point set obtained by Cunningham [20] for a 2D hexagonal lattice was used. The equations for $\alpha^{\parallel}$ and $\alpha^{\perp}$ obtained from equation (17) are not independent and the solutions were obtained numerically.

Below T_N the CEF susceptibilities have to be reformulated to account for the AFM ordering [21]. For a two-sublattice collinear AFM the CEF susceptibility is given by

$$\chi_0^{\lambda} = \frac{N g_{\lambda}^2 \beta^2 \langle S_i^{\lambda} : S_i^{\lambda}\rangle_0}{kT - 2zJ(0)(1 + \alpha^{\lambda})\langle S_i^{\lambda} : S_i^{\lambda}\rangle_0} \tag{20}$$

where the α^{λ} parameters are obtained from the solution of equation (17) after an appropriate change of sign.

The colon products $\langle S_i^{\lambda} : S_i^{\lambda}\rangle_0$ in equation (15) for Ni^{2+} were evaluated from the eigen values and functions of $\mathcal{H}_{\text{eff}}$ [22]. They are, for $D' = D - zJ(\alpha^{\parallel} - \alpha^{\perp})$

$$\langle S_i^{\parallel} : S_i^{\parallel}\rangle_0 = \frac{2e^{-D'/kT}}{1 + 2e^{-D'/kT}} \tag{21}$$

$$\langle S_i^{\perp} : S_i^{\perp}\rangle_0 = \frac{2(D'/kT)^{-1}[1 - e^{-D'/kT}]}{1 + 2e^{-D'/kT}}. \tag{22}$$

The best fits were obtained by a non-linear least-squares fitting of equation (18) to the experimental susceptibility and are shown as solid lines in figure 4. The best fit was for a value of $D/k = 16.1$ K; $J/k = -58$ K; $g_{\parallel} = 2.05$ and $g_{\perp} = 2.13$.

The calculated 2D susceptibility diverges at 260 K since the denominator in equation (18) goes to zero. This temperature, however, has no thermodynamic significance and

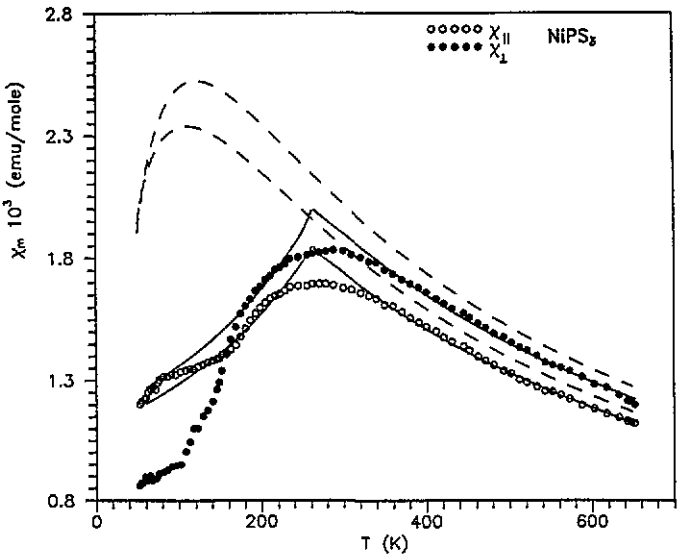

Figure 4. The anisotropic magnetic susceptibilities of $NiPS_3$ single crystals, parallel ($\chi_{\parallel}$) and perpendicular ($\chi_{\perp}$) to the trigonal axis, as a function of temperature. The solid lines are the fit of the anisotropic susceptibility expressions of equation (18) and equation (20) in the CEF approximation for $J/k = -58$ K; $D/k = 16.1$ K; $g_{\parallel} = 2.05$ and $g_{\perp} = 2.13$. The broken lines are the anisotropic susceptibilities calculated in the Oguchi approximation for the same values of J, D, $g_{\parallel}$ and $g_{\perp}$ as in the CEF approximation.

should not be compared with the experimental T_N, since magnetic ordering in the weakly XY anisotropic $NiPS_3$ arises as a consequence of weak inter-layer coupling. Below 260 K equation (20) was used to calculate the susceptibility. Since the in-layer symmetry of the low-temperature-ordered magnetic lattice is the same as that of the crystallographic lattice [3] the same set of $6k$ points was used for computing the Brillouin zone averages. Inter-layer coupling was accounted for by a molecular field. It may be seen from figure 4 that a reasonable fit is obtained between 200 K and T_N. Below T_N the fit is extremely poor and an approach using spin waves is likely to be a better approximation, but is beyond the scope of the present work. It is interesting to note that the temperature at which the CEF susceptibility diverges, 260 K, corresponds to the temperature of the experimental χ_{max}. This temperature may be interpreted as the temperature at which the in-layer staggered susceptibility is a maximum. Although the high-temperature fits in the CEF and Oguchi models (figures 1 and 4) are comparable, the CEF achieves the same quality of fit for a lower value of J. This may be clearly seen in figure 4, where the broken line is the susceptibility calculated in the Oguchi model, using the J, D and g values which gave the best fit for the CEF. The CEF formalism is superior to the Oguchi model in being able to account for short-range spin correlations; however, it too underestimates antiferromagnetic correlations near χ_{max}. The Oguchi model could in principle be improved, by considering clusters larger than a dimer for the evaluation of the effective field; this however is not particularly easy [13]. The CEF has the additional advantage of being computationally simple and consequently may be easily extended to systems with magnetic Hamiltonians more complicated than the present one.

4. Conclusions

The anisotropic susceptibilities of the layered antiferromagnet $NiPS_3$ ($T_N = 155$ K) have been measured between 45 K and 650 K. The susceptibilities show a weak XY anisotropy in the high-temperature paramagnetic phase with $\chi_\perp > \chi_\parallel$, where $\chi_\parallel$ is the susceptibility when the external field is along the trigonal axis (perpendicular to the layer). Below T_N $\chi_\parallel > \chi_\perp$. The system may be described by the effective spin Hamiltonian $\mathcal{H} = DS_{iz}^2 - \sum_{ij} J_{ij} S_i \cdot S_j$, with the quadratic single-ion anisotropy terms introducing anisotropy in an otherwise isotropic situation. The exchange J and single-ion anisotropy parameter D were determined from an analysis of anisotropic susceptibility data for two different models: (i) the Oguchi model in which a pair of spins chosen at random is treated exactly while their interactions with the rest of the crystal are approximated by a mean field and (ii) the correlated effective field (CEF) approximation developed by Lines which reduces the many-body problem to a single-particle, non-interacting ensemble form, by introducing static temperature-dependent correlation parameters, which are evaluated by forcing consistency with the fluctuation–dissipation theorem. Analytical expressions of the anisotropic susceptibilities have been derived for the Oguchi model. It is found that the CEF approximation is superior to the Oguchi model in being able to account for short-range antiferromagnetic correlation and hence gives a better description of the susceptibility in $NiPS_3$. The exchange and crystal field parameters for the CEF approximation are $J/k = -58.0$ K; $D/k = 16.1$ K; $g_\parallel = 2.05$ and $g_\perp = 2.13$.

Appendix. $\langle S_\lambda \rangle$ for an Ni^{2+} dimer with quadratic single-ion anisotropy terms

The energies and wavefunctions of the Ni^{2+} dimer in the absence of a field ($H_\parallel = H_\perp = 0$) in equation (2) are given in table A1.

Table A1. $\gamma = [(3J - D)^2 + 8JD]^{1/2}$; $C_1 = -2\sqrt{2}D/[(9J + D + 3\gamma)^2 + 8D^2]^{1/2}$ and $C_2 = (9J + D + 3\gamma)/[(9J + D + 3\gamma)^2 + 8D^2]^{1/2}$.

Wavefunctions	Energies
$\psi_{1,2} = \lvert \pm 1, \pm 1\rangle$	$E_{0,1} = E_{0,2} = -6J + 2D$
$\psi_{3,4} = \frac{1}{\sqrt{2}}(\lvert 0, \pm 1\rangle + \lvert \pm 1, 0\rangle)$	$E_{0,3} = E_{0,4} = -6J + D$
$\psi_5 = C_2\frac{1}{\sqrt{6}}(2\lvert 0, 0\rangle + \lvert 1, -1\rangle + \lvert -1, 1\rangle) + C_1\frac{1}{\sqrt{3}}(\lvert 0, 0\rangle - \lvert 1, -1\rangle - \lvert -1, 1\rangle)$	$E_{0,5} = -3J + D - \gamma$
$\psi_{6,7} = \frac{1}{\sqrt{2}}(\lvert 0, \pm 1\rangle - \lvert \pm 1, 0\rangle)$	$E_{0,6} = E_{0,7} = -2J + D$
$\psi_8 = \frac{1}{\sqrt{2}}(\lvert 1, -1\rangle - \lvert -1, 1\rangle)$	$E_{0,8} = -2J + 2D$
$\psi_9 = C_1\frac{1}{\sqrt{6}}(2\lvert 0, 0\rangle + \lvert 1, -1\rangle + \lvert -1, 1\rangle) + C_2\frac{1}{\sqrt{3}}(\lvert 0, 0\rangle - \lvert 1, -1\rangle - \lvert -1, 1\rangle)$	$E_{0,9} = -3J + D + \gamma$

$\langle S_\lambda \rangle_{\text{dimer}}$ were calculated by treating the Zeeman terms in equation (2) as a perturbation. When the field is along the z direction ($H_\parallel \neq 0$, $H_\perp = 0$) the eigen values and eigen functions are obtained from first-order perturbation theory. They are listed in table A2.

When the field is along the x or y direction ($H_\perp \neq 0$, $H_\parallel = 0$) the first-order perturbation energies are zero since $S_\perp$ does not commute with the Hamiltonian and the energies are evaluated using second-order non-degenerate perturbation theory. The energies are tabulated in table A3.

Table A2.

$E_1 = -6J + 2D - 2g_{\parallel}\beta H_{\text{eff}}$
$E_2 = -6J + 2D + 2g_{\parallel}\beta H_{\text{eff}}$
$E_3 = -6J + D - g_{\parallel}\beta H_{\text{eff}}$
$E_4 = -6J + D + g_{\parallel}\beta H_{\text{eff}}$
$E_5 = -3J + D - \gamma$
$E_6 = -2J + D - g_{\parallel}\beta H_{\text{eff}}$
$E_7 = -2J + D + g_{\parallel}\beta H_{\text{eff}}$
$E_8 = -2J + 2D$
$E_9 = -3J + D + \gamma$

Table A3.

$E_1 = E_2 = -6J + 2D + g_{\perp}^2\beta^2 H_{\text{eff}}^2 D^{-1}$
$E_3 = E_4 = -6J + D - g_{\perp}^2\beta^2 H_{\text{eff}}^2\left(D^{-1} + \dfrac{3C_2^2}{6J - 2\gamma} + \dfrac{3C_1^2}{6J + 2\gamma}\right)$
$E_5 = -3J \bullet D - \gamma + \dfrac{3g_{\perp}^2\beta^2 H_{\text{eff}}^2 C_2^2}{3J - \gamma}$
$E_6 = E_7 = -2J + D - g_{\perp}^2\beta^2 H_{\text{eff}}^2 D^{-1}$
$E_8 = -2J + 2D + g_{\perp}^2\beta^2 H_{\text{eff}}^2 D^{-1}$
$E_9 = -3J + D + \gamma + \dfrac{3g_{\perp}^2\beta^2 H_{\text{eff}}^2 C_1^2}{3J + \gamma}$

The ensemble average of the spin moment of the dimer $\langle S_\lambda\rangle_{\text{dimer}}$ is given by

$$\langle S_\lambda\rangle_{\text{dimer}} = \frac{kT}{g_\lambda\beta}\frac{\delta \ln Z_\lambda}{\delta H} \tag{A1}$$

$$Z = \sum_{i=1}^{9} e^{-E_i/kT}$$

where E are the energies of the dimer in the applied field. For a small value of H_{eff} second-order terms in H may be dropped and the expression for $\langle S_\lambda\rangle_{\text{dimer}}$ is

$$\langle S_\parallel\rangle_{\text{dimer}} = \frac{2g_\parallel\beta H_\parallel}{kT}\frac{(4e^{4J-D/kT} + e^{4J/kT} + 1)}{G(J, D, T)} \tag{A2}$$

where

$$G(J, D, T) = 2e^{4J-D/kT} + 2e^{4J/kT} + 2 + e^{J+\gamma/kT} + e^{J-\gamma/kT} + e^{-D/kT}$$

$$\langle S_\perp\rangle_{\text{dimer}} = \frac{2g_\perp\beta H_\perp F(J, D, T)}{G(J, D, T)} \tag{A3}$$

wherein

$$F(J, D, T) = D^{-1}[-2e^{4J-D/kT} + 2e^{4J/kT} + 1 - e^{-D/kT}] + \frac{3C_2^2}{3J - \gamma}(e^{4J/kT} - e^{J+\gamma/kT})$$

$$+ \frac{3C_1^2}{3J + \gamma}(e^{4J/kT} - e^{J-\gamma/kT}).$$

References

[1] De Jongh L J and Miedema A R 1974 *Adv. Phys.* **23** 1
[2] Willet R D, Gatteschi D and Kahn O (ed) 1985 *Magneto Structural Correlations in Exchange Coupled Systems* (Dordrecht: Reidel)
[3] Brec R 1986 *Solid State Ion.* **22** 3
[4] Clement R, Lomas L and Audiere J P 1990 *Chem. Mater.* **2** 641
[5] Joy P A and Vasudevan S 1992 *J. Am. Chem. Soc.* **114** 7792
[6] Joy P A and Vasudevan S 1993 *Chem. Mater.* **5** 1182
[7] Le Flem G, Brec R, Ouvrard G, Louisy A and Segransen P 1982 *J. Phys. Chem. Solids* **43** 455
[8] Joy P A and Vasudevan S 1992 *Phys. Rev.* B **46** 5425
[9] Joy P A and Vasudevan S 1992 *Phys. Rev.* B **46** 5134
[10] Carlin R L 1986 *Magneto-Chemistry* (Berlin: Springer)
[11] Lines M E 1974 *Phys. Rev.* B **9** 3927
[12] Oguchi T 1955 *Progr. Theor. Phys.* **13** 148
[13] Smart J S 1966 *Effective Field Theories of Magnetism* (Philadelphia, PA: Saunders)
[14] Cruse D A and Gerloch M 1977 *J. Chem. Soc. Dalton Trans.* 152
[15] Mabbs F E and Machin D J 1973 *Magnetism and Transition Metal Complexes* (London: Chapman and Hall)
[16] Abragam A and Bleaney B 1970 *EPR of Transition Ions* (Oxford: Clarendon)
[17] Lines M E and Eibschütz M 1975 *Phys. Rev.* B **11** 4853
[18] Eibschütz M, Lines M E and Sherwood L C 1975 *Phys. Rev.* B **11** 4595
[19] Chadi D J and Cohen M L 1973 *Phys. Rev.* B **8** 5947
[20] Cunningham S L 1974 *Phys. Rev.* B **10** 4988. The wavevectors (in units of π/a) for the 2D hexagonal lattice along with the weighting factors are $(\frac{2}{9}, 2/9t)$, $\frac{1}{9}$; $(\frac{4}{9}, 4/9t)$, $\frac{1}{9}$; $(\frac{8}{9}, 8/9t)$, $\frac{1}{9}$; $(\frac{2}{3}, 2/9t)$, $\frac{2}{9}$; $(\frac{8}{9}, 4/9t)$, $\frac{2}{9}$; $(\frac{10}{9}, 2/9t)$, $\frac{2}{9}$. $t = \sqrt{3}$
[21] Nugmanov A I and Tagirov L R 1992 *J. Magn. Magn. Mater.* **111** 301
[22] Lines M E 1975 *Phys. Rev.* B **9** 3766